

## Using of vacuum insulated tandem accelerator for perspective materials irradiation by a fast neutron flux

Yaroslav Kolesnikov <sup>a,b,\*</sup>, Marina Bikchurina <sup>a,b</sup>, Timofey Bykov <sup>a,b</sup>, Dmitrii Kasatov <sup>a,b</sup>, Nataliia Singatulina <sup>a,b</sup>, Ivan Shchudlo <sup>a,b</sup>, Evgeniia Sokolova <sup>a,b</sup>, Victor Bobrovnikov <sup>a</sup>, Sergey Gromilov <sup>b,c</sup>, Aleksandr Sukhikh <sup>b,c</sup>, Darya Klyamer <sup>b,c</sup>, Andrey Shoshin <sup>a,b</sup>, Alexander Burdakov <sup>a,d</sup>, Alexey Ovsienko <sup>e</sup>, Sergey Taskaev <sup>a,b</sup>

<sup>a</sup> Budker Institute of Nuclear Physics, 11 Lavrentiev ave., 630090 Novosibirsk, Russia

<sup>b</sup> Novosibirsk State University, 2 Pirogov str., 630090 Novosibirsk, Russia

<sup>c</sup> Nikolaev Institute of Inorganic Chemistry, 630090 Novosibirsk, Russia

<sup>d</sup> Novosibirsk State Technical University, 20 Karl Marx ave., 630073 Novosibirsk, Russia

<sup>e</sup> Virial Ltd, Russia

### ARTICLE INFO

#### Keywords:

Vacuum insulated tandem accelerator

Perspective materials

Radiation testing

Fast neutrons

Dosimetry

### ABSTRACT

Radiation testing of perspective materials by fast neutron flux is an important task for large physical facilities such as the Large Hadron Collider or the International Thermonuclear Experimental Reactor. Such a source of fast neutrons is the accelerator based neutron source VITA, proposed, developed and actively used at the Budker Institute of Nuclear Physics. The paper describes the accelerator based neutron source VITA, its features related to the generation of a powerful fast neutron flux, the result of a long lasting experiment with fast neutron generation, further plans to increase the energy and current of the deuteron beam, to develop a compact fast neutron generator, and to increase the total fast neutron yield to  $2 \cdot 10^{13} \text{ s}^{-1}$ . The paper presents results of the perspective materials irradiation by fast neutrons flux.

### 1. Introduction

The electrostatic tandem accelerator of an original design Vacuum Insulated Tandem Accelerator (VITA) [1] has been proposed and developed at the Budker Institute of Nuclear Physics (BINP). It is the first part of the accelerator based neutron source VITA [2], others are lithium target for generating stable neutron with total yield up to  $2 \cdot 10^{12} \text{ n/s}$  and set of beam shaping assemblies for achieving neutrons with desired spectrum – from cold to fast. The neutron source has applications in various fields, such as: boron neutron capture therapy (BNCT) [3,4], activation studies of materials, blistering studies of materials [5], fundamental studies of the physics issues, radiation testing of perspective materials and other applications. Radiation testing of the perspective materials is providing by fast neutrons, which are generated in the process of exothermic (non-threshold) reaction  $^7\text{Li}(\text{d},\text{n})$  [6].

Neutrons are used for various applications. In the case of radiation testing of materials at least  $10^{13}$ – $10^{14}$  neutrons per  $\text{cm}^2$  must be accumulated on the material to be tested, for which the neutron flux density

must be at least  $10^8$ – $10^9 \text{ cm}^{-2}\text{s}^{-1}$ . Neutrons are also used to perform nuclear doping of silicon, for this purpose  $10^{14}$ – $10^{18}$  neutrons must be accumulated per  $1 \text{ cm}^2$  of material, nuclear reactors are used for this. Neutrons are also used for small angle scattering, diffractometry, spectrometry, reflectometry, mechanical stress studies, magnetic and crystalline structure studies of materials. For these purposes, the required neutron flux density is  $10^5$ – $10^6 \text{ cm}^{-2}\text{s}^{-1}$ . The VITA, as will be shown later, fulfills these conditions, and occupies a median position between total neutron yield (or flux density) and compactness and simplicity of operation and maintenance.

### 2. Materials and methods

#### 2.1. VITA and lithium target

The VITA provides dc proton/deuteron beam with a wide range of beam energy and current. Accelerator based neutron source VITA consists of the vacuum insulated tandem accelerator for obtaining a high-

\* Corresponding author at: 11 Lavrentiev ave., 630090 Novosibirsk, Russia.

E-mail address: [Ya.A.Kolesnikov@inp.nsk.su](mailto:Ya.A.Kolesnikov@inp.nsk.su) (Y. Kolesnikov).

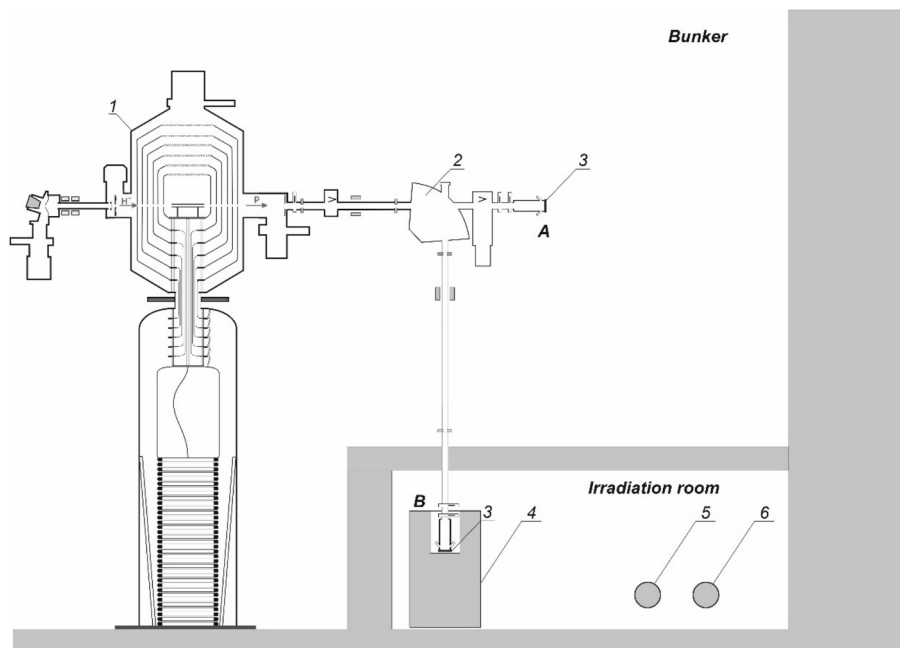


**Fig. 1.** Scheme of the VITA in the fast neutron generating mode: 1 – vacuum insulated tandem accelerator, 2 – bending magnet, 3 – lithium target, 4 – neutron concentrator, 5 –  $\gamma$ -dosimeter, 6 – neutron dosimeter, A and B – lithium target placement positions.

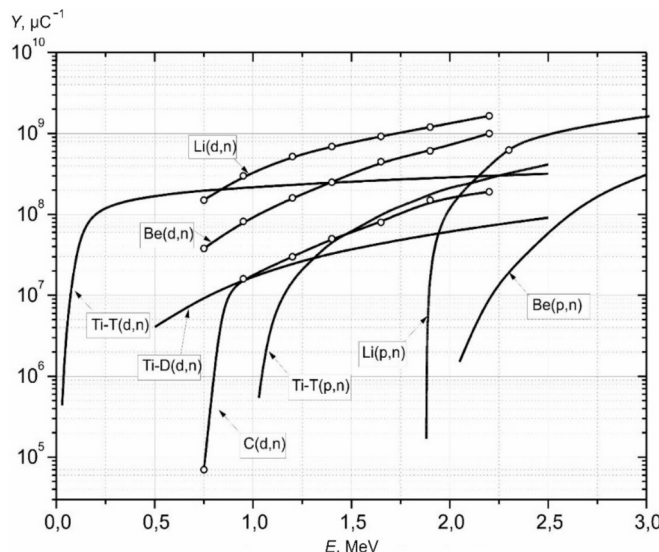


**Fig. 2.** Neutron yield of reactions in thick targets.

power dc proton/deuteron beam, the lithium target for generating neutrons and a set of beam shaping assemblies for obtaining neutrons with required energy – cold ( $D_2O$  moderator at cryogenic temperature), thermal ( $D_2O$  or plexiglass), epithermal ( $MgF_2$  moderator), fast (concentrator without moderation).

The scheme of the facility in the fast neutron generating mode is shown in Fig. 1. Negative ion beam ( $H^-$  or  $D^-$ ) is accelerated in the high-voltage electrodes of vacuum insulated tandem accelerator 1, stripped in the argon stripping target to positive ion beam ( $p^+$  or  $d^+$ ) and accelerated again to the energy up to 2.3 MeV. The lithium target 3 is located in the vertical or horizontal path, to transport ion beam to the position A the bending magnet 2 is not enabled; to transport ion beam to position B the bending magnet is enabled with a current, corresponding to the beam energy. When radiation tests of the materials by the fast neutrons are conducted, the target is located in the position B in the irradiation

room, neutron concentrator 4 is located around the lithium target. The  $\gamma$ -5 and neutron 6 dosimeters are located at the distance of 5 m from the lithium target to stay in the working regime.

## 2.2. B. Neutron generating reactions

Radiation resistance tests require neutrons with an energy of more than 1 MeV, which are obtained in the following exothermic reactions:

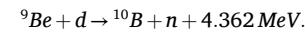
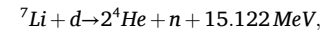
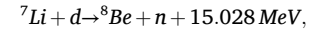
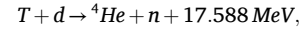
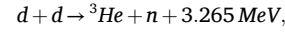


Fig. 2 presents neutron yields obtained in these and other reactions in thick targets [7]. Reaction  $Li(d,n)$  has the highest neutron yield when the energy of deuterons exceed 0.8 MeV. Indeed, at a beam energy of 2 MeV neutron yields in  $Be(d,n)$  and  $Li(p,n)$  reactions are  $6 \times 10^{11}$  and  $1.1 \times 10^{11} \text{ mC}^{-1}$  respectively, while in the  $Li(d,n)$  reaction is  $13.5 \times 10^{11} \text{ mC}^{-1}$  [7,8].

Let us focus on the interaction of lithium with deuteron. Their interaction at a deuteron energy of 1 MeV is characterized by ten different reactions, five of them are neutron-generating:

1.  ${}^7Li + d = {}^8Be + 15.028 \text{ MeV} \rightarrow 2\alpha + 0.094 \text{ MeV};$
2.  ${}^7Li + d = n + \alpha + \alpha + 15.121 \text{ MeV};$
3.  ${}^7Li + d = \alpha + {}^5He + 14.162 \text{ MeV} \rightarrow n + \alpha + 0.957 \text{ MeV};$
4.  ${}^6Li + d = {}^7Be + 3.385 \text{ MeV};$
5.  ${}^6Li + d = {}^3He + {}^5He + 0.840 \text{ MeV} \rightarrow n + \alpha + 0.957 \text{ MeV}.$

Using a diamond detector and an  $\alpha$ -spectrometric complex based on a silicon semiconductor detector, we measured the cross-sections of reactions 1, 2 and 3 of the deuteron-lithium interaction with neutron generation, all reactions with the lithium-7 isotope, the results are presented in [9,10].



**Fig. 3.** Photos of the lithium target assembly (left) and concentrator (right).

We have not measured the remaining two reactions. In the future, it is possible to measure the cross-section of reaction 4 by measuring activated berillium-7 on a lithium target, and reaction 5 using a proton filter with an energy of up to 1 MeV in the  $\alpha$ -spectrometric complex.

Nevertheless, the knowledge we have gained is sufficient to state that when generating fast neutrons, it is recommended to use a target enriched with lithium-7, since neutron-generating reactions of lithium-7 and deuterium are the most productive. Knowing the reaction cross section it is known that it is possible to reconstruct not only the total neutron yield from the target, but also the neutron energy spectrum, which will undoubtedly be useful in future experiments on the generation of fast neutron flux.

The important part of radiation tests of materials is possibility to detect and measure/simulate/estimate quantity and distribution of the neutrons. The VITA equipped with neutron detector with GS-20 lithium glass for measuring of the neutron flux; set of activation foils; two HPGe-detectors for measuring spectrum and flux of the  $\gamma$ -rays;  $\alpha$ -spectrometers for measuring elemental composition by spectroscopy of ion scattering;  $\gamma$ -dosimeters for measuring of the radiation fields during and after irradiation.

### 3. Experimental facility and results

#### 3.1. Performance of VITA

Earlier it was shown that VITA can be used as fast neutrons generator with total neutron yield  $1.4 \times 10^{12} \text{ s}^{-1}$  [6] and this yield is sufficient for providing radiation testing of materials, fast neutron therapy [11] and other applications.

After this, the irradiation room was prepared (position B of the lithium target in the Fig. 1) for decreasing the neutrons dose rate outside the bunker and in the control room. Walls of this room are made of concrete with boron carbide, door made of borated polyethylene, these materials are effective moderators and absorbers of neutrons. Inside the room, around the lithium target a concentrator was made. The concentrator is made of lead and wood, since lead is a reflector of neutrons and wood is not activating by neutrons. Photos of the lithium target assembly and concentrator are shown in Fig. 3. Lithium target consists of copper disc with diameter 144 mm and 3 mm thickness. On this copper disc the lithium is deposited by thermal heating method in vacuum chamber of lithium deposition system of BINP.

Since preparations were finished, the fast neutrons irradiation experiment have been resumed. There were different experimental groups that were irradiating following devices:

- coils of optical cables developed at the Saclay Nuclear Research Center (France) for high-luminosity operation of the CERN Large Hadron Collider (LHC);
- semiconductor photomultipliers and direct current converters for the ATLAS detector of the CERN LHC;
- diamond neutron detector for the International Thermonuclear Experimental Reactor (ITER, Cadarache, France);
- plates made of B<sub>4</sub>C for ITER (Cadarache, France);
- neodymium magnets for the hybrid focusing system of the DARIA in the Institute for Theoretical and Experimental Physics ITEP (Moscow) [12];
- natural and synthetic diamonds for the Nikolaev Institute of the Inorganic Chemistry (Novosibirsk).
- gas sensors based on titanyl phthalocyanines for Novosibirsk State University laboratory;
- semiconductor devices of the Novosibirsk Semiconductor Devices Factory.

When the neutrons are generated by the proton beam, the energy of the beam is varied up to 2.3 MeV and current up to 10 mA. In case of the deuteron beam, these values smaller. The energy of the beam is limited by the power supply of bending magnet down to 1.5 MeV. The current of the beam is limited by the ion-optical system of the H- source down to 1.5 mA. These current and energy provide generation of fast neutrons with a total yield of  $10^{12} \text{ s}^{-1}$ .

Before delivering a powerful deuteron beam (with  $\sim$ MeV energy and  $\sim$ mA current) a calibration of neutron flux was conducted, since  $\gamma$ -dosimeter cannot properly work in the radiation fields, dose rate of which exceeds 0.1 Sv/h. Using the neutron area monitor UDMN-100 (SPC Doza) [13], it was established, that at the energy of the deuteron beam 1.011 MeV and current 0.5  $\mu$ A the dose rate of the generated neutrons is 0.044 Sv/h. Distance from the lithium target to sensitive area of detector was 120 mm. It was also measured, that the increase of the energy of the deuteron beam from 1.0 to 1.5 MeV increases neutron dose rate twice. Since the amount of generated neutrons is proportional to the beam current, finally, at the deuteron beam energy 1.5 MeV and current 1.5 mA the neutron dose rate at the distance of 120 mm from the lithium

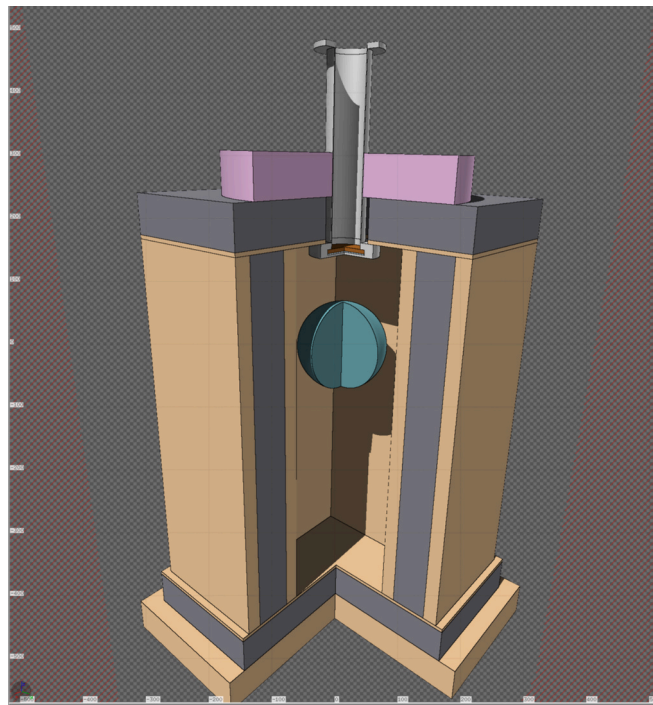


Fig. 4. Example of the geometry model for FLUKE code simulation.

target is  $\approx 250$  Sv/h. Also, computer simulations based on FLUKA [14] were performed to estimate dose level. Obtained difference between the experimental data and the simulation is about 10 %. Example of geometry description in the simulation (lead concentrator with wooden

housing, target and sphere is UDMN-100) shown at the Fig. 4.

Additionally, spectrum of the  $\text{Li}(\text{d},\text{n})$  reaction at energy 1.5 MeV was measured by our team using AT1117M Radiation Monitor with BDKN-06 Detection Unit and a set of spherical moderators with diameters 3", 3.5", 4", 4.5", 5", 6", 7", 8", 9", 9.5", 10", 12" (Atomtex, Republic of Belarus) [15]. Since spherical moderators have different diameters, they have different sensitive areas, which allows estimating spectrum. Measurements of this set were reconstructed in energy spectrum using sensitive curves of spherical moderators. Reconstructed spectrum in logarithmic and linear scales are shown at the Fig. 5.

The experiment was paused for a construction of a temporary wall, made of concrete blocks, containing boron carbide for neutron capturing. The photo of the outside view of the bunker is shown at the Fig. 6.

After these preparations the neutron dose rate in the control room became  $\sim 4$   $\mu\text{Sv}/\text{h}$ , this level is acceptable for radiation group A personnel.

After the experiment restart, the facility was working average 11 h per day (8 h in neutron generation mode), 5 days a week, from 25th April to 25th May of 2022 year. During this time, it was only one unexpected stop, when we had to substitute malfunctioned forevacuum pump by a working one. In the Fig. 7 the neutron yield (in arbitrary units) normalized on deuteron current as a function of time (sec) in 2nd and 23th irradiation day, measured by neutron detector with lithium glass GS-20 (The Saing-Gobain Crystals, USA) is shown.

The total integral current on the surface of the lithium target was  $122 \text{ mA} \times \text{h}$ , the maximum neutron flux density per sample unit reached  $2.9 \times 10^{14} \text{ cm}^{-2}$ . After the accumulated deuteron current integral of  $122 \text{ mA} \times \text{h}$ , there were no any degradation of the neutron yield – nor deuteron energy degradation, nor degradation of the lithium neutron generating target.

After the prolonged irradiation, the studied samples and materials

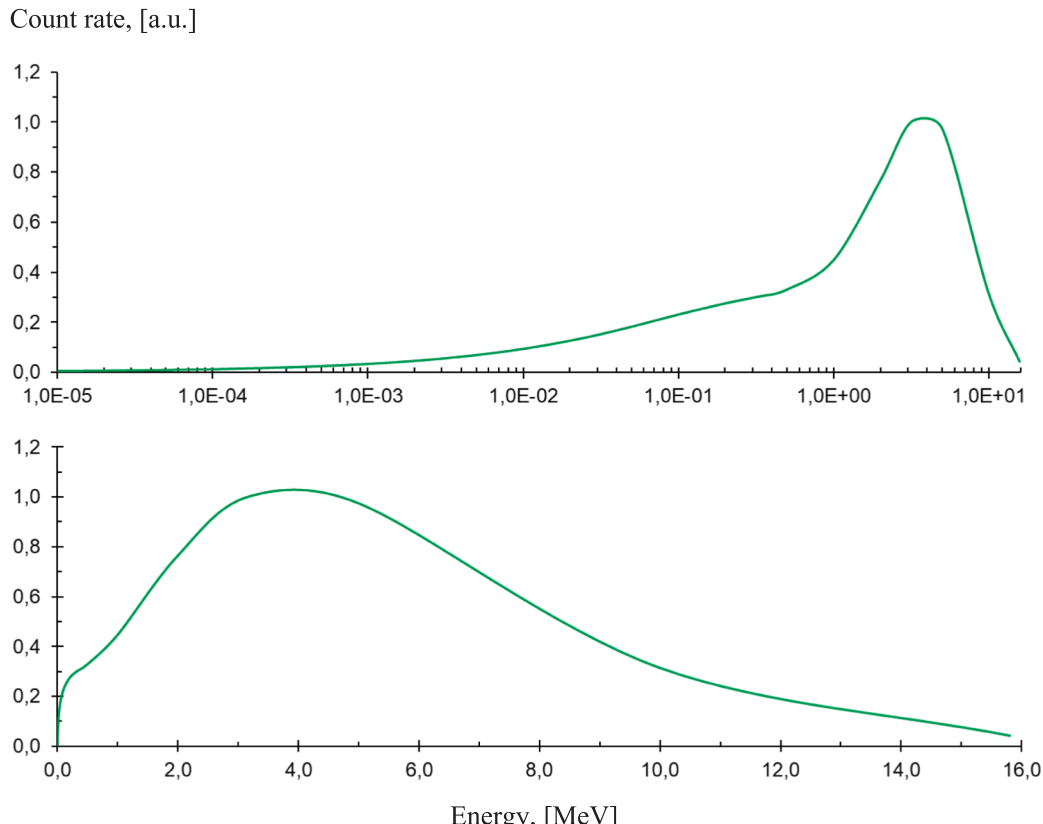
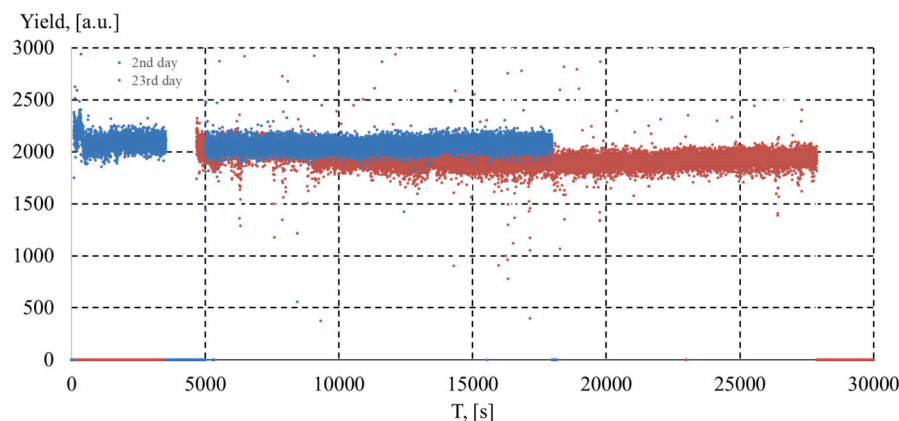


Fig. 5. Spectrum of the  $\text{Li}(\text{d},\text{n})$  reaction at deuteron beam energy 1.5 MeV, measured by a AT1117M Radiation Monitor with BDKN-06 Detection Unit and a set of spherical moderators. Top curve is in logarithmic scale, bottom curve in linear scale.



**Fig. 6.** Photo of the outside view of the bunker. This neutron protection wall contains boron for neutron capture to decrease neutron dose rate outside the bunker.



**Fig. 7.** Neutron yield (arb. unit) normalized on deuteron current as a function of time (sec) in 2nd (blue curve) and 23th (red curve) irradiation day, measured by neutron detector with lithium glass GS-20 (The Saint-Gobain Crystals, USA).

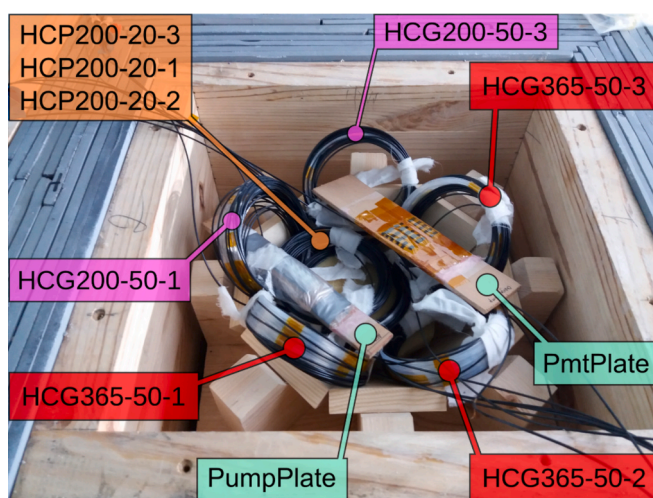


**Fig. 8.** Location of the optical coils cables and semiconductor photomultipliers inside the concentrator.

were cooled for approximately 1 week in the irradiation room. This was due not to the significant activation of the samples but to the high activation of the lithium target and the radiation hazard for the staff.

**Table 1**

Neutron flux densities on irradiated objects with deuteron beam energy 1.5 MeV and current 1 mA.

Object	Neutrons, $[10^8 \text{ cm}^{-2}\text{s}^{-1}]$
HCP-200-20-1	3.31
HCP-200-20-2	2.24
HCP-200-20-3	5.39
HCG365-50-1	1.4
HCG365-50-2	2.31
HCG365-50-3	2.58
HCG200-50-1	1.23
HCG200-50-3	1.58
PmtPlate	4.57
PumpPlate	1.31

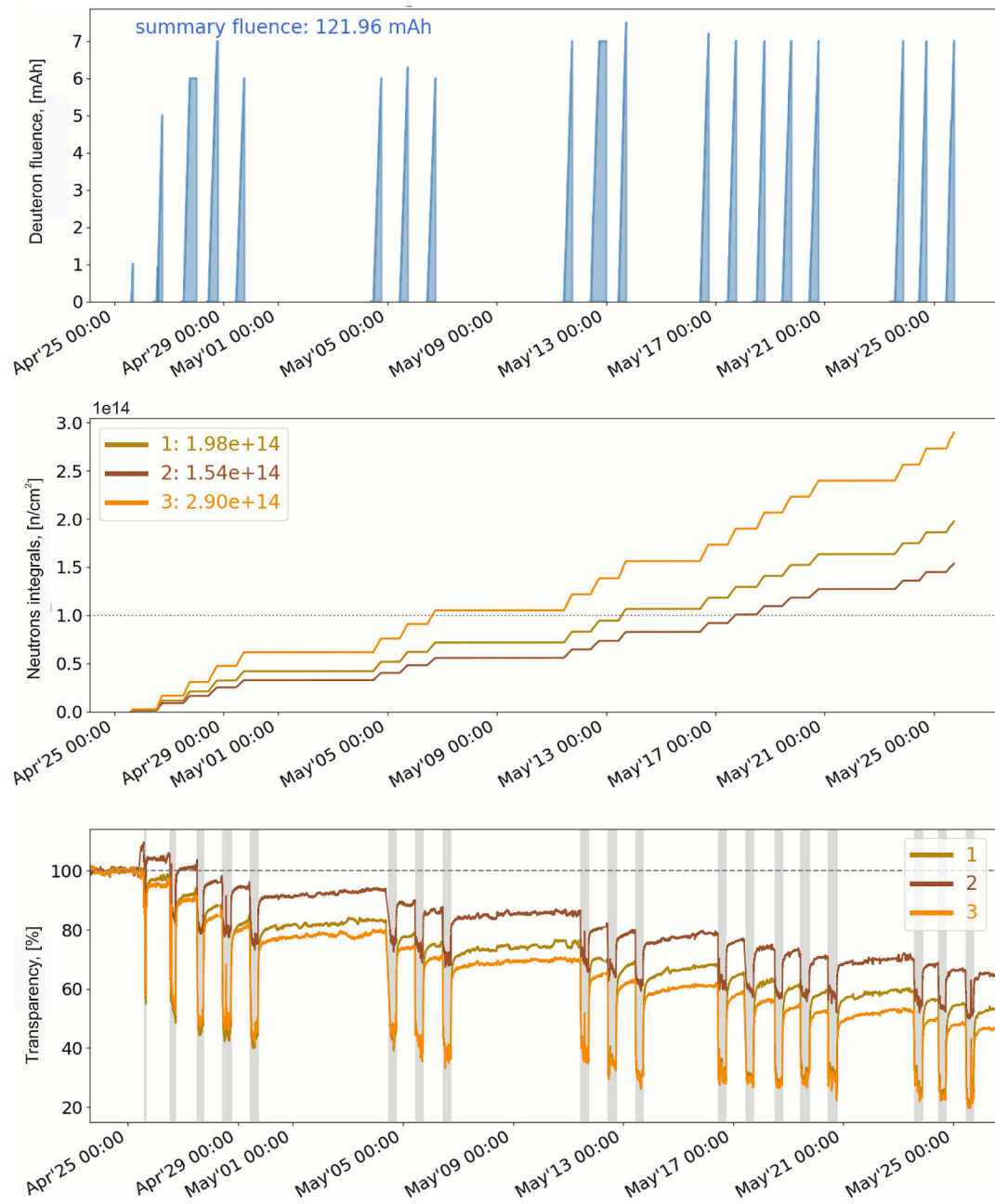


**Fig. 9.** Results of coils of optical cables for high-luminosity operation of CENR LHC irradiation. Top graph – deuteron beam fluence during working sessions of VITA, middle graph – neutrons/cm<sup>2</sup> integrals from the beginning of the irradiation on the three different optical coils, bottom graph – transparency of these irradiated samples.

### 3.2. Materials irradiation results

#### 3.2.1. Optical cables

Before discussing results of optical cables irradiation, let us take focus on some details of irradiation. Site of materials, located inside the concentrator (Fig. 3, right), is shown at the Fig. 8.

Using FLUKA simulation and calibration of the neutron area monitor UDMN-100 we obtained neutron flux densities values for these materials, values are presented in the Table 1. These calculations were made with deuteron beam energy 1.5 MeV and current 1 mA.

In the Fig. 9 dependencies of the working sessions of VITA, fast neutrons integrals on samples and the dependence of the transparency of three types of optical fiber provided by the Saclay Center for Nuclear Research (France) are shown. It has been found that the transparency of an optical fiber decreases by  $\sim 50\%$  as soon as the fiber is irradiated with

fast neutrons, and does not return to its previous level after the end of irradiation. The measured degradation of transparency of optical fibers varies from 20 % to 35 % with a fast neutron fluence of  $10^{14} \text{ n/cm}^2$ .

Such a detailed study of the dependence of optical fiber transparency on fast neutron fluence has been performed for the first time, and the results obtained are unique and important for science and practice, including laser calibration of the CMS detector calorimeter during the planned operation of the CERN Large Hadron Collider in the high-luminosity mode.

#### 3.2.2. Boron cabide

The BINP, Institution Project Center ITER, and ITER Organization cooperatively prepared and agreed on a specification for boron carbide for diagnostic ports (ITER\_D\_457TBH) [16,17]. There are very strict requirements for ceramics: the outgassing rate is limited to  $1 \cdot 10^{-8}$

**Table 2**

Degradation of mechanical properties of sintered boron carbide ceramics produced by Virial Ltd. after irradiation by fast neutrons with fluence  $10^{14} \text{n/cm}^2$ .

	After	Before
Density, $\text{g/cm}^3$	$2.14 \pm 0.02$	$2.26 \pm 0.01$
Young's modulus $E$ , GPa	$365 \pm 14$	$420 \pm 7$
Bending strength $\sigma$ , MPa	$190 \pm 13$	$220 \pm 11$

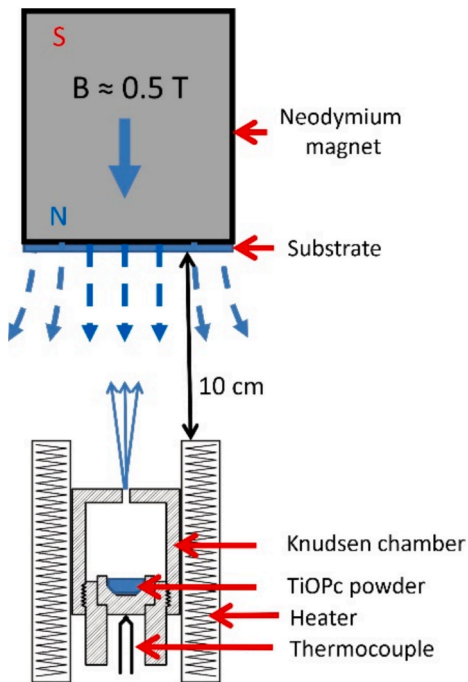


Fig. 10. Setup for the thin TiOPc layers deposition.

$\text{Pa} \cdot \text{m}^3 \cdot \text{s}^{-1} \cdot \text{m}^{-2}$  for hydrogen at  $100^\circ\text{C}$ . Vacuum tests of the first delivery batch showed that sintered ceramics produced by Virial Ltd. meet these requirements.

First, the VITA facility was used for experiments on the activation of ceramics by thermal neutrons. The  $\gamma$ -ray spectra after irradiation of ceramics with thermal neutrons contained mainly manganese lines. By comparing the intensity of manganese lines in ceramics from different manufacturers and a 316L-IG steel sample containing 1.83 % Mn, irradiated simultaneously with the ceramic samples, the concentration of manganese in the ceramics was determined. The manganese content of the ceramics was in the range of 0.0001–0.0003 % [18].

The activation of ceramics after irradiation with fast neutrons at the VITA accelerator was then measured. The flux density was  $3 \cdot 10^9 \text{ neutrons} \cdot \text{cm}^{-2} \cdot \text{s}^{-1}$  for 20 min and the cumulated fluence was  $3.6 \cdot 10^{12} \text{ neutrons} \cdot \text{cm}^{-2}$ . Which roughly corresponds to the conditions inside the EP11, where the characteristic neutron fluxes are  $10^8 \div 10^{11} \text{ neutrons} \cdot \text{cm}^{-2} \cdot \text{s}^{-1}$  [16]. Radioactivity levels have been shown to drop rapidly within three days of activation [16].

Next, the ceramics were subjected to prolonged fast neutron (average energy 5.68 MeV) exposure to study the degradation of mechanical properties and demonstrate resistance to cracking. Dust formation is especially important due to the location of optical diagnostics in the diagnostic ports [15]. Ceramics was tested with a fluence of  $10^{14} \text{ n/cm}^2$  (corresponding to 2–200 ITER shots for Diagnostic Shield Module at EP11, depending on the block's distance from the plasma). Not one sample cracked. Mechanical strength decreased by 15 %, Table 2.

Based on the test results, a conclusion was made about the applicability of ceramics in ITER diagnostic ports, and estimates were also made about the degree of boron burnup during ITER operation [14].

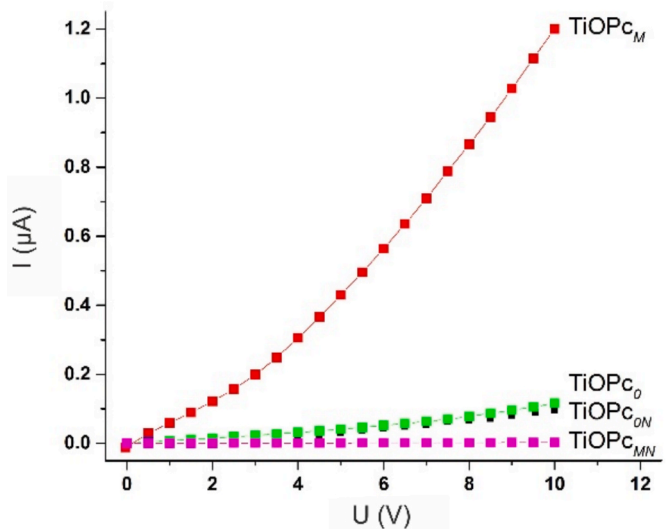


Fig. 11. Current-voltage characteristics of TiOPcM and TiOPc0 layers and TiOPcMN and TiOPcON layers irradiated by fast neutrons.

Based on the Manufacturing and Inspection Plan and test results, an End of manufacturing report on the first delivery batch (ITER\_D-DAGDG6) has been prepared and approved by the ITER Organization, allowing the ceramics to be used for delivery as part of the ports to the ITER site. In total, Virial Ltd. has already produced more than 54 thousand blocks of boron carbide ceramics for ITER diagnostic ports.

### 3.2.3. Titanyl phthalocyanine (TiOPc) layers

Among numerous organic semiconductors, metal phthalocyanines (Mpc) are particularly interesting due to their high thermal and chemical stability and unique electronic properties. The ability of MPC to sublimate in vacuum allows preparing thin homogeneous highly oriented polycrystalline layers by vacuum thermal evaporation, which is increasingly often used in not only the production of field – effect transistors, solar cells, diodes, etc., but also as active layers of chemical sensors [19]. The TiOPc layers were deposited using Knudsen chamber, as it shown at Fig. 10. Deposition time of the layers was 1 h with heater temperature  $450^\circ\text{C}$ . On this stage there were two types of TiOPc, – prepared with applying magnet field of  $\sim 0.5 \text{ T}$  (TiOPcM) and without magnetic field (TiOPc0).

After irradiation by fast neutrons on the VITA, the current–voltage characteristics of four TiOPc layers groups were measured. These groups are TiOPcM, TiOPc0, which were defined earlier, and TiOPcMN, TiOPcON, which were irradiated by fast neutrons with a fluence of  $3 \cdot 10^{14} \text{ cm}^{-2}$ . Measurement results are shown in Fig. 11.

First difference of the prepared materials is the result of evaporation. Samples evaporated with using magnets has more conductivity. Results after neutron irradiation are that TiOPcMN conductivity decreased by two orders of magnitude and TiOPcON conductivity not changed.

## 4. Conclusion

Accelerator based neutron source VITA as generator of fast neutrons is a reliable facility. Nowadays the total yield of generated fast neutrons is  $10^{12} \text{ s}^{-1}$ . Research has shown that VITA as a fast neutron generator can operate for at least a month in the 5 days a week, 8 h a day regime of neutron generation.

The compact fast neutron source now is under development. It will generate  $\sim 10^{12}$  fast neutrons per second. This is sufficient for providing investigations on radiation testing of perspective materials for large physical facilities, such as CERN, ITER etc.

The accelerator based neutron source VITA is currently undergoing modernization, which will allow the transport of a powerful (up to 50

kW/cm<sup>2</sup>) deuteron beam to a rotating lithium target to reach a total neutron yield of  $\sim 2 \times 10^{13}$ s<sup>-1</sup>. Such a flux makes VITA the brightest neutron source with neutron concentration 10<sup>4</sup> cm<sup>-3</sup> and allow to provide direct studies of neutron structure using lepton or hadron beams or even construct an n-n collider.

## CRediT authorship contribution statement

**Yaroslav Kolesnikov:** Writing – original draft, Investigation. **Marina Bikchurina:** Investigation, Formal analysis. **Timofey Bykov:** Software, Investigation. **Dmitrii Kasatov:** Investigation. **Nataliia Sinyatulina:** Formal analysis. **Ivan Shchudlo:** Investigation. **Evgeniia Sokolova:** Formal analysis. **Victor Bobrovnikov:** Validation, Investigation. **Sergey Gromilov:** Investigation, Formal analysis. **Aleksandr Sukhikh:** Formal analysis. **Darya Klyamer:** Formal analysis. **Andrey Shoshin:** Investigation, Formal analysis. **Alexander Burdakov:** Investigation. **Alexey Ovsienko:** Investigation. **Sergey Taskaev:** Writing – review & editing, Supervision, Conceptualization.

## Funding

This research was funded by Russian Science Foundation, grant number 19-72-30005, <https://rscf.ru/project/19-72-30005/>.

## Declaration of competing interest

The authors declare that they have no known competing financial interests or personal relationships that could have appeared to influence the work reported in this paper.

## Data availability

Data will be made available on request.

## References

- [1] S. Taskaev, Accelerator based Neutron Source VITA, FizMatLit, Moscow, 2024.
- [2] S. Taskaev, E. Berendeev, M. Bikchurina, T. Bykov, D. Kasatov, I. Kolesnikov, A. Koshkarev, A. Makarov, G. Ostreinov, V. Porosev, S. Savinov, I. Shchudlo, E. Sokolova, I. Sorokin, T. Sycheva, G. Verkhovod, Neutron source based on vacuum insulated tandem accelerator and lithium target, Biology 10 (350) (2021), <https://doi.org/10.3390/biology10050350>.
- [3] M. Dymova, S. Taskaev, V.E. Richter, E. Kuligina, Boron neutron capture therapy: current status and future perspectives, Cancer Commun. 40 (2020) 406–442, <https://doi.org/10.1002/cac2.12089>.
- [4] Advances in Boron Neutron Capture Therapy. International Atomic Energy Agency, Vienna, Austria. 2023. ISBN: 978-92-0-132723-9.
- [5] A. Badruttinov, T. Bykov, S. Gromilov, Y. Higashi, D. Kasatov, Ia Kolesnikov, A. Koshkarev, A. Makarov, T. Miyazawa, I. Shchudlo, E. Sokolova, H. Sugawara, S. Taskaev, In situ observations of blistering of a metal irradiated with 2-MeV protons, Metals 7 (558) (2017), <https://doi.org/10.3390/met7120558>.
- [6] D. Kasatov, A. Koshkarev, A. Makarov, G. Ostreinov, S. Taskaev, I. Shchudlo, A Fast-neutron source based on a vacuum-insulated tandem accelerator and a lithium target, Instrum. Experim. Tech. 63 (5) (2020), <https://doi.org/10.1134/S0020441220050152>.
- [7] V. Kononov, M. Bokhovko, O. Kononov, Accelerator based neutron sources for medicine, in: Proc. of International Symposium on Boron Neutron Capture Therapy, 2004, pp. 62–68.
- [8] C. Lee, X.-L. Zhou, Thick target neutron yields for the  $7\text{Li}(p, n)7\text{Be}$  reaction near threshold, Nucl. Instrum. Meth. Phys. Res. Sect. B: Beam Int. Mater. Atoms 152 (1) (1999) 1, [https://doi.org/10.1016/S0168-583X\(99\)00026-9](https://doi.org/10.1016/S0168-583X(99)00026-9).
- [9] S. Taskaev, M. Bikchurina, T. Bykov, D. Kasatov, Ia Kolesnikov, G. Ostreinov, S. Savinov, E. Sokolova, Measurement of cross-section of the  $6\text{Li}(d, \alpha)4\text{He}$ ,  $6\text{Li}(d, p)7\text{Li}$ ,  $6\text{Li}(d, p)7\text{Li}^*$ ,  $7\text{Li}(d, \alpha)5\text{He}$ , and  $7\text{Li}(d, n)4\text{He}$  reactions at the deuteron energies from 0.3 MeV to 2.2 MeV, Nucl. Inst. Meth. Phys. Res. B 554 (2024) 165460, <https://doi.org/10.1016/j.nimb.2024.165460>.
- [10] S. Meshchaninov, A. Krasilnikov, N. Rodionov, Yu. Kashchuk, S. Obudovsky, A. Dzhurik, T. Kormilitsyn, R. Rodionov, V. Amosov, G. Nemtsev, M. Bikchurina, T. Bykov, G. Verkhovod, D. Kasatov, Ya. Kolesnikov, G. Ostreinov, E. Sokolova, S. Taskaev, Measurement of cross-section of the  $7\text{Li}(d, n)8\text{Be}$  reactions at the deuteron energies from 0.4 to 2.1 MeV, Phys. At. Nucl. 87 (6) (2024) S771–S785, <https://doi.org/10.1134/S1063778824700789>.
- [11] K. Gordon, I. Gulidov, T. Fatkhudinov, S. Koryakin, A. Kaprin, Fast and furious: fast neutron therapy in cancer treatment, Int. J. Part. Therapy 9 (2) (2022) 59–69, <https://doi.org/10.14338/IJPT-22-00017>.
- [12] I. Kilmetova, A. Kozlov, G. Kropachev, T. Kulevoy, D. Liakin, O. Sergeeva, V. Skachkov, Yu. Stasevich, Hybrid quadrupole lens for the focusing channel of the DARIA complex, J. Surf. Invest. 17 (2023) 772–777, <https://doi.org/10.1134/S1027451023040067>.
- [13] [https://www.doza.ru/catalog/continuous\\_monitoring/UDMN-100/](https://www.doza.ru/catalog/continuous_monitoring/UDMN-100/).
- [14] <https://fluka.cern/>.
- [15] <https://atomtex.com/en/at1117m-radiation-monitor-bdkn-06-detection-unit-and-set-spherical-modulators>.
- [16] A. Shoshin, A. Burdakov, M. Ivantsivskiy, S. Polosatkin, A. Semenov Yu Sulyaev, E. Zaitsev, P. Polozova, S. Taskaev, D. Kasatov, I. Shchudlo, M. Bikchurina, Test results of boron carbide ceramics for ITER port protection, Fus. Eng. Design 168 (2021), <https://doi.org/10.1016/j.fusengdes.2021.112426>.
- [17] A. Shoshin, A. Burdakov, M. Ivantsivskiy, R. Reichle, V. Uditsev, J. Guirao, S. Pak, A. Zvonkov, D. Kravtsov, N. Sorokina, Y. Sulyaev, A. Listopad, D. Gavrilenko, A. Taskaev, E. Shabunin, V. Seryomin, S. Shiyankov, E. Zaytcev, P. Seleznev, A. Semenov, S. Polosatkin, S. Taskaev, D. Kasatov, I. Shchudlo, M. Bikchurina, V. Modestov, A. Smirnov, A. Pozhilov, A. Lobachev, I. Loginov, O. Shagniev, I. Kirienko, I. Buslakov, Integration of ITER diagnostic ports at the Budker Institute, Fus. Eng. Design 178 (2022) 113114, <https://doi.org/10.1016/j.fusengdes.2022.113114>.
- [18] A. Shoshin, A. Burdakov, M. Ivantsivskiy, S. Polosatkin, M. Klimenko, A. Semenov, S. Taskaev, D. Kasatov, I. Shchudlo, A. Makarov, N. Davydov, Qualification of boron carbide ceramics for use in ITER ports, IEEE Trans. Plasma Sci. 48 (6) (2020) 1474–1478, <https://doi.org/10.1109/TPS.2019.2937605>.
- [19] S. Dyusenova, D. Klyamer, A. Sukhikh, I. Shchudlo, S. Taskaev, T. Basova, S. Gromilov, Influence of magnetic field on the structure and sensor properties of thin titanyl phthalocyanine layers, J. Struct. Chem. 64 (3) (2023) 337–346, <https://doi.org/10.1134/S0022476623030010>.